Research paper

Analysis of the bearing resistance of the modified bolted end-plate joints of thin-walled profiles used in modular construction

Karol Prałat[1], Arkadiusz Plis[2]

Abstract: The paper presents the results of testing the bearing resistance of the bolted joints of thin-walled profiles used in modular construction. The two types of joints currently applied in the construction industry were subjected to tests. One of them served as the reference sample, and the other as the research sample, which was used to find a solution that is more favorable in terms of the complexity of its production process and its bearing resistance. In addition to the modified shape of the end-plates, the bearing resistance of the joint was also analyzed with regards to the different diameters of bolts (bolts M12 and M16 were used), their classes (the difference between bolts of class 8.8 and 10.9 was examined), and also the number of them in the joint (3 or 5 bolts). Moreover, two thicknesses of steel sheets (3 mm and 4 mm), from which thin-walled cold-bent profiles were made, were used in the research. The bearing resistance tests were carried out with the use of a testing press of the authors' own design. On the basis of the measurements, plots of the dependence between the deflection of the samples and the force acting in the middle of their span were drawn. It was shown that the tested profile joint had an increased bearing resistance by up to 26% when compared to the reference sample. The maximum destructive bending moment M was equal to 10.7 kN·m for the reference sample, and to 13.5 kN·m for the analyzed design solution. In total, 6 types of modified joints were made for the tests, of which five showed a comparable or higher bearing resistance than the reference sample. Each type of joint was tested by bending it in two directions in relation to the central axis of its cross-section.

Keywords: bearing resistance, modular construction, modular structure nodes, thin-walled profiles

---

[1]DSc., PhD., Eng., Warsaw University of Technology, Faculty of Civil Engineering, Mechanics and Petrochemistry, Łukasiewicza 17, 09-400 Płock, Poland, e-mail: Karol.Pralat@pw.edu.pl, ORCID: 0000-0001-5116-0379
[2]M.Sc. Eng., Warsaw University of Technology, Faculty of Civil Engineering,Mechanics and Petrochemistry, Łukasiewicza 17, 09-400 Płock, Poland, e-mail: arkadiusz.plis.dokt@pw.edu.pl, ORCID: 0000-0002-9384-0679

1. Introduction

Modular constructions are more and more valued by builders, as well as by the users of such structures. Prefabricated modules are not just technical containers, portable exhibition pavilions, or office pavilions, but also structures with repeated units, i.e. public utility buildings such as schools, kindergartens, hospitals, hotels and residential houses [1–5]. In recent years they have also been used in high-rise constructions [6–8].

The main advantage of these types of constructions is the time of completing an investment. If necessary, modular buildings can be moved to different places, dismantled, and reassembled, and thanks to the system of their construction, it is possible to expand facilities in any configuration. The manufacturing of modules takes place in production plants, where the conditions for their formation are controlled, which in turn guarantees the quality of building elements. Due to this, production works are possible all year round, regardless of the weather. In addition, in Australia, Great Britain, Singapore and the United States, there is a growing trend of using modular construction. This is due to the fact that this method of production is cheaper and faster than traditional construction, which is of great importance in the context of the shortage of housing in these countries [9]. Modular construction, although quite often used in low-rise buildings [10], has not yet been widely applied in high-rise buildings. The use of modular construction in high-rise buildings is currently limited to a level of less than 1% [11]. This is due to the lack of knowledge regarding the implementation of such technologies in high-rise buildings, the lack of design guidelines, the lack of module joining techniques, and the insufficient understanding of the behavior of such a structure (its global stability, and its bearing resistance).

Design or material solutions are constantly being developed for modular construction, and innovative solutions are being sought in order to increase the bearing resistance of the resulting structures [11–14]. In modular construction, screw connections of thin-walled profiles are often used. Bolted end-plate joints are nowadays very often used in steel structures and are applied in the contact joints of whole elements or their parts.

Bolted end-plate joints are often used in frame structures, with the computational load calculations of such joints being analyzed in the second half of the 19th century. However, the lack of appropriate tools for the analysis of a structure, as well as the applied simplifications, did not allow for a wide development of this field of science. Research was mainly limited to the calculations of welded joints, because in such connections, stress distributions can be easily determined [15].

The first studies concerning bolted end-plate joints mainly focused on joints for pipe cross-sections [16–18]. In these works, the authors noted that the occurrence of moments in two planes only affects the rotation of the neutral axis, and this in turn has an influence on the lever arms of the internal forces related to individual bolts. In the considered cases, the impact of moments on the bearing resistance of individual bolts in the node was not taken into account. Paper [19] describes the analysis of the bolted joints of I-section elements. The studies were mainly related to the anchoring of columns, or the connections of beams with reinforced concrete columns. In turn, the connections of beams with columns, which were loaded with a bending moment that was perpendicular to the plane of the frame, were analyzed in papers [20, 21].

The bearing resistance of end-plate joints during bending mainly depends on the bearing resistance of the bolts located in the rows closest to the tensioned flange of the beam. The ultimate limit state of a bending end-plate joint involves the breaking of a bolt in the joint. If it is assumed that the end-plates in the joint are sufficiently rigid (thick), then the design moment resistance $M_{j,Rd}$ of the end-plate joint has the following form (1.1):

$$(1.1) \qquad M_{j,Rd} = \sum_r h_r F_{tr,Rd}$$

where: $F_{tr,Rd}$ – the effective design tension resistance of bolt-row r, h_r – distance from bolt-row r to the centre of compression, r – bolt-row number.

End-plate joints are equipped with end-plates, and are used, among others, in the joints and nodes of solid frames, where they transfer bending moments and tensile longitudinal forces (Fig. 1). The direction of the main component of the load is then parallel to the axis of the connectors. Unstressed end-plate joints transfer the internal forces in the joint by tensioning the bolts. The pre-stressing (controlled tightening of the bolt nuts) of these joints allows for the transmission of tensile loads by reducing the pressure (compressive) stresses in the joint between the end-plates. Therefore, end-plate joints are characterized by low deformability and high strength.
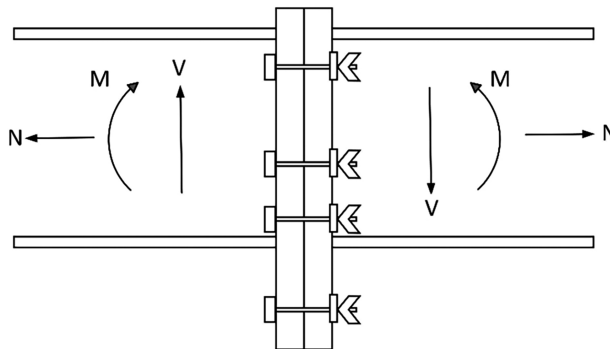
Fig. 1. An example of a bolted end-plate joint and a diagram of its loading

Due to the existence of leverage effect forces and the deformability of a joint's components, the assessment of the bearing resistance of end-plate joints during bending is complex. The design principles that are included in PN-EN 1993-1-8 [22] only apply to unidirectionally loaded end-plate joints. Therefore, designers often face the problem of how to take into account the effect of the secondary moment on the bearing resistance of the joint in the plane of the frame. Most often, additional connectors are used to transfer the bending moment from the plane of the frame. However, due to the configuration of the joint, these connectors may be additionally loaded with a moment in the plane of the frame, and the resultant forces in the connectors may exceed their bearing resistance. Paper [15] presents a proposal of how to calculate bolted end-plate joints loaded with moments in two planes. Two methods of calculating such connections are presented: the resultant bending moment method, and the force summation method.

Other types of bolted connections that are used in steel structures are lap joints, which are widely described in literature [23–25], but are not often applied in modular objects frames. This especially applies to modular objects frames involving container designs, which is due to fact that in such case bolts should be hidden inside the profiles (columns).

In the case of steel structures and their joints in modular construction, an additional difficulty is caused by the use of thin-walled cold-formed profiles with an asymmetrical cross-section and unpredictable behavior under loading. Moreover, the need to maintain limited external and internal dimensions of a single module can also pose a problem. Due to the lack of defined rules for the design of such joints, laboratory tests and advanced engineering software that uses the finite element method are used in such cases.

The aim of the study was to analyze the bearing resistance of the end-plate joints of thin-walled profiles that are currently used in modular construction, and also to find the most favorable solution in terms of the complexity of the production process and the bearing resistance of such joints. In addition to the modified shape of the connection between profiles, an analysis of bolted end-plate joints during bending was also performed with regards to the number of used bolts and their class, as well as to the different thicknesses of the profile's metal sheets.

2. Experimental procedures

2.1. Materials

Seven different types of thin-walled bolted end-plate joints were prepared for the research (Table 1). Type 1 was the reference sample, and types 2.1–4.2 were modified joints with variable parameters, such as: the number and class of the used bolts, and the thickness of the metal sheets of the thin-walled profiles. All the types of joints were made in six repetitions.

Table 1. Types of samples used in the bearing resistance tests

Type	Number and diameter of bolts	Bolt class	Sheet thickness of joined profiles [mm]	External dimensions of joined profiles [mm]	Thickness of end-plates [mm]
1	$3 \times M12$	8.8	4	180×150	10
2.1	$3 \times M12$	8.8	4	180×150	12
2.2	$3 \times M12$	10.9	4	180×150	12
3.1	$5 \times M12$	8.8	4	180×150	12
3.2	$5 \times M12$	10.9	4	180×150	12
4.1	$5 \times M12$	8.8	3	180×150	12
4.2	$3 \times M12$	8.8	3	180×150	12

All the samples were made in the Prefabrication Department of Modular System Sp. z o.o. (limited liability company). The connected 3 mm and 4 mm thick profiles were made of S355MC cold forming steel, while the 12 mm end-plates and 10 mm top and bottom plates were made of S355J2 steel. All the used metal plates, of the same thickness, came from one delivery batch. Fig. 2 shows a detailed scheme of the reference sample. The joined profiles were made of 4 mm thick metal sheet, while the end-plates and top and bottom plates were 10 mm thick. The samples were 1000 mm long, and the joints were placed in the center of their span. Three M12×40 class 8.8 bolts with a hexagonal head, which were tightened with a torque wrench (with a torque of 90 N·m), were used in the joints. The prepared sample consisted of two parts. In the first one, the end-plate of the bolted joint was welded directly to the profile that had dimensions of $180 \times 150 \times 4$ mm. In the second part, the end-plate was welded to a steel angle section with a thickness of 5 mm, and this section was then assembled to the profile.
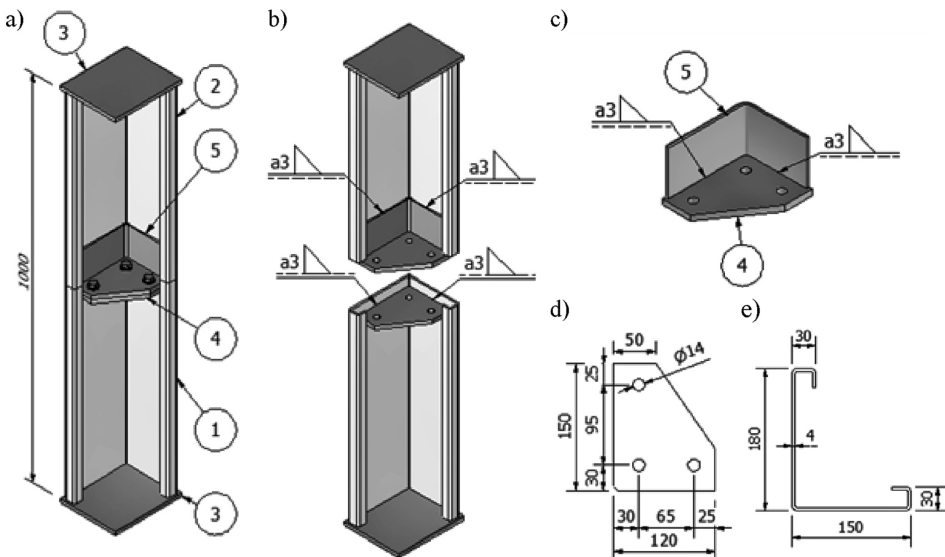
Fig. 2. The reference sample (type 1) used in the research: a), b) view of sample: 1, 2 – 180×150×4 mm profiles; 3 – top and bottom plates (190 × 160 × 10 mm); 4 – 10 mm end-plates with ϕ 14 mm holes; 5 – 5 mm thick steel angle section; c) view of element welded to the upper profile, d) plate welded to the bottom profile, e) cross-section of the joined profiles

The scheme of prepared samples 2.1–4.2 is shown in Fig. 3. The joined profiles were made of 3 mm or 4 mm metal sheets, while the end-plates were 12 mm thick. The samples were made of two parts. In the first part, the end-plate had threaded holes with a diameter of 12 mm, and the second part had non-threaded holes with a diameter of 14 mm. The joints were made using three or five M12×35 socket head cap bolts, without the use of washers and nuts. The 8.8 and 10.9 class bolts were tightened with a torque wrench using a torque of 90 N·m. All the tested samples, when compared to the reference sample, differed

with regards to their modified end-plate. Due to the much lower labor consumption and complexity of the 2.1–4.2 type joints (reference type of joint requires more material, more welding and is more complicated in prefabrication because end-plates need to be placed in a certain distance from the element end before welding), the aim of the study was to find such a configuration of these joints that would allow a load capacity of no lower than that of the type 1 joint to be obtained.
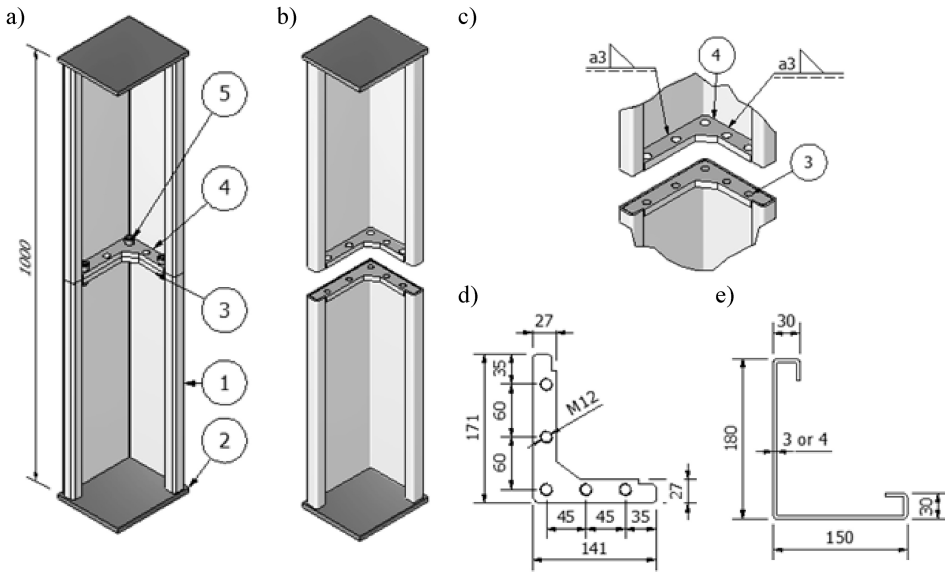
Fig. 3. Modified samples (types 2.1 to 4.2) used in the research: a), b) view of sample: $1 - 180 \times 150 \times 4$ mm or $180 \times 150 \times 3$ mm profiles, $3 - 12$ mm thick end-plate with threaded holes, $4 -$ end-plate with non-threaded holes of ϕ 14 mm, $5 -$ M12 bolts with a socket head cap, c) end plate welds d) detail of element welded to the upper and bottom profile of a modified end-plate e) cross-section of the joined thin-walled profiles

2.2. Experimental setup

During the experiment, the samples were tested by subjecting them to bending, with the applied force and the measured deflection then being recorded. Each type of connection was tested in a state of unidirectional bending in two positions: with the vertical positioning of the longer flange, and also with the vertical positioning of the shorter flange of the profile. Each test was performed so that the maximum tensile force occurred in the most outer bolt. The force was applied so that the axis of its action was as close as possible to the shear center in order to minimize the influence of the moment in the profile. In the case of using asymmetrical profiles, the shear center is outside their cross-section. The scheme of loading and arranging the samples is shown in Fig. 4. The tested samples were not mounted at their ends, but instead a free support scheme was used.
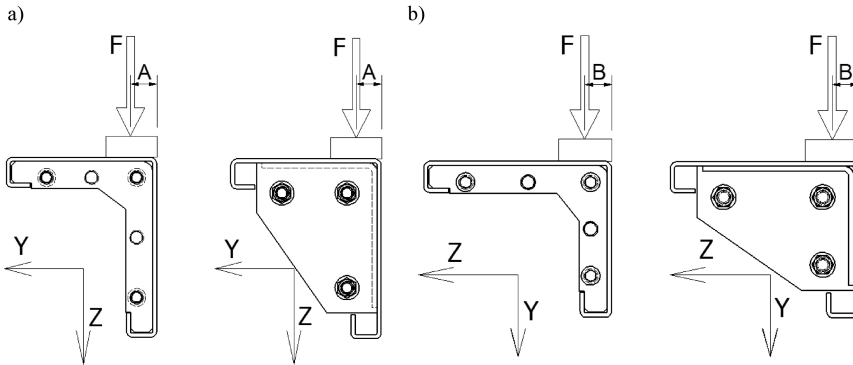
Fig. 4. Scheme of the arrangement of the samples in reference to Y and Z axes and the application of force F: a) vertical arrangement of the longer flange of the profile, force position: $A = 25$ mm, bending about Y axis, b) horizontal arrangement of the longer flange of the profile, force position: $B = 25$ mm, bending about Z axis

For the purpose of the experimental research, a hydraulic press was made in the production departments of Modular System Sp. z o.o. (limited liability company) according to the authors' own design (Fig. 5). The test stand consisted of: a strength press frame (element 1 in Fig. 5), adjustable support (element 2) the tested sample (element 3), and KEMMLER strain gauges with a measuring range of 0–50 mm and an accuracy of 0.01 mm mounted in the middle of the sample span.
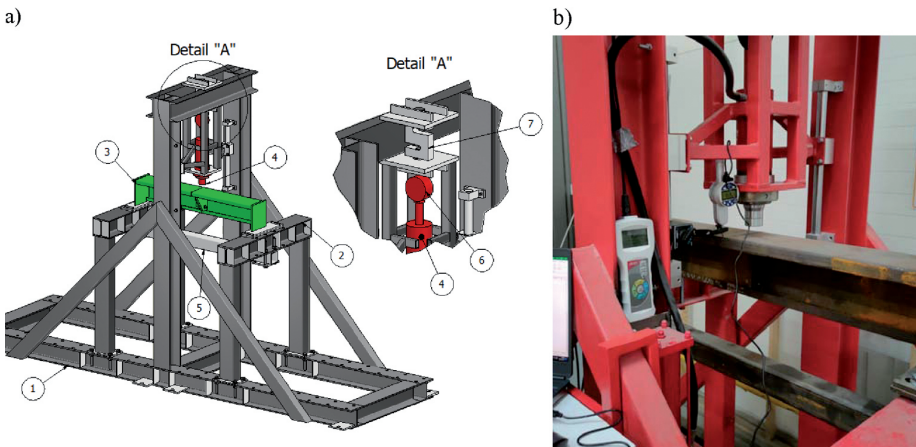
Fig. 5. Experimental setup: a) design model, b) setup during the tests. 1 – steel frame of the press, 2 – adjustable support, 3 – tested sample, 4 – 20T actuator, 5 – profile for attaching the deformation measuring gauges, 6 – digital manometer, 7 – AXIS FB50k force meter

The strength press used an actuator (with a maximum pressure of 20 tons) with a pneumatic-hydraulic pump, and also a force gauge with an external AXIS FB50k force

meter (with a measuring range of up to 75 kN and a reading unit of 10 N – element 7). Additional control of the acting force was conducted by installing a SIKA E2 digital manometer on the actuator (element 6). It had a measuring range of up to 40 MPa and an accuracy of 0.01 MPa. Using formula (2.1), it was possible to calculate the force generated by the F_S actuator:

$$(2.1) \qquad F_S = p \cdot (S_D - S_d)$$

where: F_S – the force generated by the actuator [N], p – hydraulic pressure [Pa], S_D – the piston's surface area [m^2], S_d – the piston rod's surface area [m^2].

The force and deflection were read and recorded by connecting the gauges to a computer. Measurements were made until the samples were destroyed, i.e. the breaking of the most outer bolts, or the moment when the sample's material was plasticized and it was impossible to reach a further load value increase. Deflection value was registered for each 1 kN of the force increment.

3. Results and discussion

As a result of the research, force-deflection diagrams for the individual types of joints were obtained in the case of bending in two independent directions. Moreover, the maximum forces acting on each type of joint at the moment of their failure (Table 2 and Table 3), as well as the form of failure, were determined. Measured destructive forces were used for calculating the bending moment, according to the formula (3.1) and formula (3.2):

$$(3.1) \qquad M_{Yi} = (F_{Zi}/2) \cdot L/2$$

$$(3.2) \qquad M_{Zi} = (F_{Yi}/2) \cdot L/2$$

where: M_{Yi} – bending moment about Y axis [kN·m], F_{Zi} – Force acting in axis Z [kN], M_{Zi} – bending moment about Z axis [kN·m], F_{Yi} – Force acting in axis Y [kN], L – sample length (1.0 m for each sample).

For each investigated sample, the destructive moments about both axes: M_Y, M_Z were presented in tables. Also, for each type of connection, the mean values of destructive force: $\overline{x}_{FZ}$, $\overline{x}_{FY}$ and moment: $\overline{x}_{MY}$, $\overline{x}_{MZ}$, as well as the standard deviations of forces: σ_{FZ}, σ_{FY} and moment: σ_{MY}, σ_{MZ}, were shown. In the last column of tables, for every connection type, there was calculated the percentage ratio of destructive force mean value in relation to the value obtained for reference sample (connection type 1).

Based on the data in Table 2, it can be observed that in the tested type 2.1 joint, the destructive force (acting in the direction of the greater stiffness of the joined profiles) was almost equal to the force that was measured in the case of the reference samples. In both cases, three M12 bolts of class 8.8 were used in the joint. Changing the class of bolts to class 10.9 resulted in an increase in the average destructive force by almost 7%. In turn, the use of five M12 bolts resulted in an increase in the average force by almost 20% and 26% for the class 8.8 and 10.9 bolts, respectively, when compared to the reference sample.

Table 2. Values of forces and bending moments acting on the samples at the moment of the joint's failure – testing in the direction of the greater stiffness of the cross-section (bending about Y axis)

Type	Sample No.	Destructive force F_Z [kN]	$\bar{x}_{FZ}$ [kN]	σ_{FZ} [kN]	Destructive moment M_Y [kN·m]	$\bar{x}_{MY}$ [kN·m]	σ_{MY} [kN·m]	$\bar{x}_{FZi}/\bar{x}_{FZ1}$ [%]
1	1	42.8			10.7			
	2	42.1	42.8	0.6	10.5	10.7	0.2	100.0
	3	43.6			10.9			
2.1	7	43.9			11.0			
	8	42.7	43.0	0.7	10.7	10.7	0.2	100.3
	9	42.3			10.6			
2.2	13	47.3			11.8			
	14	44.8	45.7	1.1	11.2	11.4	0.3	106.8
	15	45.1			11.3			
3.1	19	49.9			12.5			
	20	52.6	51.3	1.1	13.2	12.8	0.3	119.8
	21	51.5			12.9			
3.2	25	55.2			13.8			
	26	54.2	54.0	1.0	13.6	13.5	0.3	126.1
	27	52.7			13.2			
4.1	31	50.1			12.5			
	32	47.9	48.4	1.2	12.0	12.1	0.3	113.1
	33	47.3			11.8			
4.2	37	35.5			8.9			
	38	34.1	34.3	0.9	8.5	8.6	0.2	80.2
	39	33.4			8.4			

When changing the thickness of the sheets from which the profiles were made (from 4 to 3 mm), the destructive force was 13% higher in the case of using five M12 bolts of class 8.8, and 20% smaller in the case of using 3 bolts, when compared to the samples of the type 1 joint.

On the basis of Table 3, it was observed that in the tested joint of type 2.1, the destructive force acting in the direction of the lower stiffness of the joined profiles was almost equal to the force measured in the reference sample. In the type 2.2 samples, the average force was higher by more than 7%, and in the type 3.1 and 3.2 samples, it was higher by 21.8% and 26.8%, respectively, when compared to the reference sample. As was the case during the tests in the direction of the greater stiffness, when the thickness of the sheets from which

Table 3. Values of forces and bending moments acting on the samples at the moment of joint's failure – testing in the direction of lower cross-sectional stiffness (bending about Z axis)

Type	Sample No.	Destructive force F_Y [kN]	$\bar{x}_{FY}$ [kN]	σ_{FY} [kN]	Destructive moment M_Z [kN·m]	$\bar{x}_{MZ}$ [kN·m]	σ_{MZ} [kN·m]	$\bar{x}_{FYi}/\bar{x}_{FY1}$ [%]
1	4	35.2			8.8			
	5	33.8	33.8	1.1	8.5	8.5	0.3	100.0
	6	32.4			8.1			
2.1	10	35.7			8.9			
	11	33.6	34.0	1.3	8.4	8.5	0.3	100.6
	12	32.7			8.2			
2.2	16	37.2			9.3			
	17	36.8	36.4	0.9	9.2	9.1	0.2	107.6
	18	35.1			8.8			
3.1	22	42.4			10.6			
	23	40.8	41.2	0.9	10.2	10.3	0.2	121.8
	24	40.3			10.1			
3.2	28	41.4			10.4			
	29	43.3	42.9	1.1	10.8	10.7	0.3	126.8
	30	43.9			11.0			
4.1	34	38.3			9.6			
	35	36.2	37.2	0.9	9.1	9.3	0.2	110.1
	36	37.1			9.3			
4.2	40	26.6			6.7			
	41	27.7	27.7	0.9	6.9	6.9	0.2	81.9
	42	28.7			7.2			

the profiles were made was changed from 4 to 3 mm, a 13% higher destructive force was observed in the case of using five M12 bolts of 8.8 class, and a 20% smaller destructive force was recorded when using three bolts (when compared to the reference sample).

Fig. 6 and Fig. 7 show the dependence between the deflection of the sample and the force acting on it for the type 1 joint (reference sample).

The tested samples of the type 1 joint were damaged as a result of the interaction of the opening of the joint, the plasticization of the plates, and the plasticization of the most outer bolt (samples 1 and 6), or due to the breaking of the most outer bolt (other samples). The critical load point of the joint (read as a point on the graph where the force-deflection curve ceases to be linear) was observed for the force value of 22 kN in the case of bending
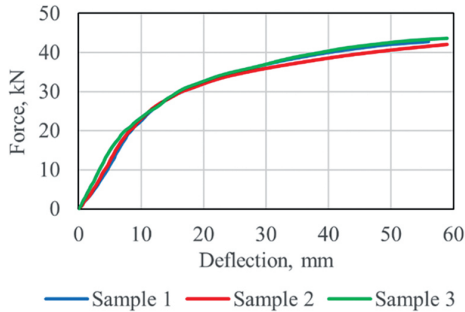
Fig. 6. Force – deflection curves for the type 1 joint. Bending about Y axis
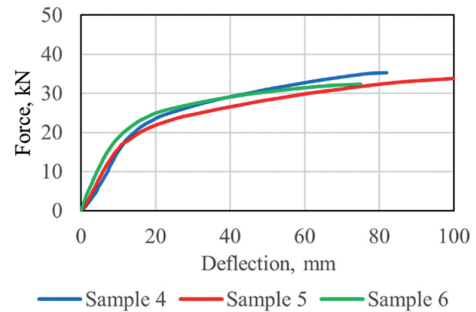
Fig. 7. Force – deflection curves for the type 1 joint. Bending about Z axis

in the direction of the greater stiffness (about Y axis) of the cross-section, and for the force value of 18 kN in the direction of lower stiffness (about Z axis).

Fig. 8 shows photos of the damaged type 1 joints. Fig. 9 and Fig. 10 show the dependence between the deflection of the tested samples and the force acting on them for the type 2.1 joints.

(a)

(b)

Fig. 8. Samples of the type 1 joint: (a) failure due to plasticization of the plates and the braking of the most outer bolt, (b) plasticization of the plates and the most outer bolt

Fig. 11 shows pictures of the damaged joints of type 2.1, which in the case of samples 9 and 12 resulted from the interaction of the opening of the joint, the plasticization of the joint plates, and the breaking of the bolt's thread, and in the case of the remaining samples – the breaking of the most outer bolt. The critical load point of the joint was observed for the force values of 25 kN and 20 kN in the case of bending in the direction of the higher and lower cross-sectional stiffness, respectively.

Fig. 12 and Fig. 13 show the dependence between the deflection of the samples and the force acting on them for the next type of joint (type 2.2). In this case, the critical load point of the joints was designated for the force value of 31 kN for bending in the direction of
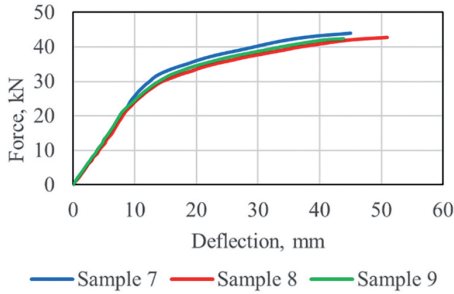
Fig. 9. Force – deflection curve for the type 2.1
joint. Bending about Y axis
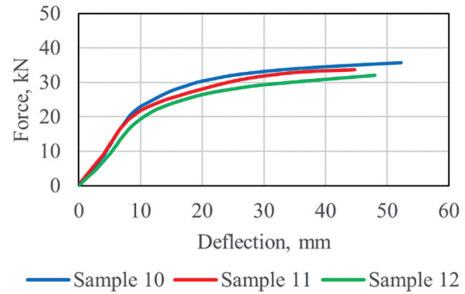
Fig. 10. Force – deflection curve for the type
2.1 joint. Bending about Z axis

(a)

(b)

Fig. 11. Samples of the type 2.1 joint: (a) failure due to plasticization of the plates and the breaking
of the thread of the most outer bolt, (b) opening of the joint plates after failure
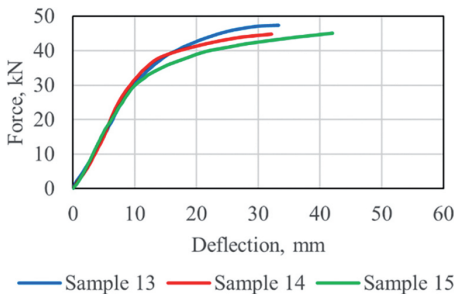
Fig. 12. Force – deflection curve for the type
2.2 joint. Bending about Y axis
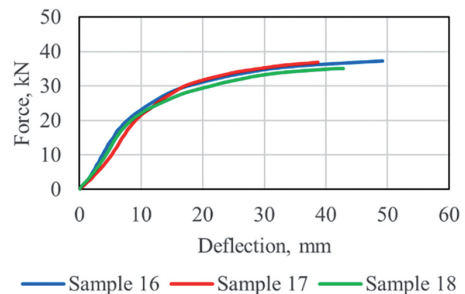
Fig. 13. Force – deflection curve for the type
2.2 joint. Bending about Z axis

greater stiffness (about Y axis), and for the force value of 20 kN for bending in the direction
of lower stiffness (about Z axis).

The type 2.2 joint samples were damaged due to the opening of the joint, the plasti-
cization of the end-plates, and the breaking of the thread of the bolt (sample No. 13), or

due to the breaking of the most outer bolt (other samples). Fig. 14 shows the samples after testing.

(a)   (b)
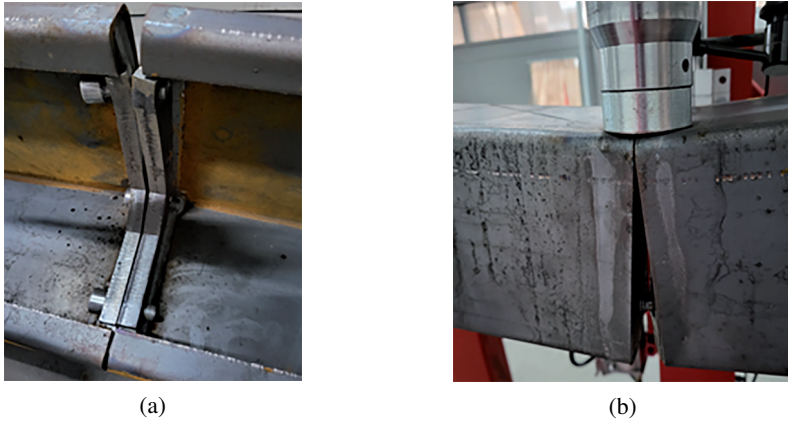
Fig. 14. Samples of the type 2.2 joint: (a) failure due to the plasticization of the end-plates and the breaking of the thread of the most outer bolt, (b) opening of the joint plates after failure

Fig. 15 and Fig. 16 show the dependence between the deflection of the tested samples and the force acting on them for the 3.1 type joints. Samples 19, 22, 23 and 24 were destroyed as a result of the interaction of the opening of the joint and the plasticization of the end-plates and the most outer bolts. In turn, the remaining samples were destroyed due to the plasticization of the end-plates and the breaking of the most outer bolt.
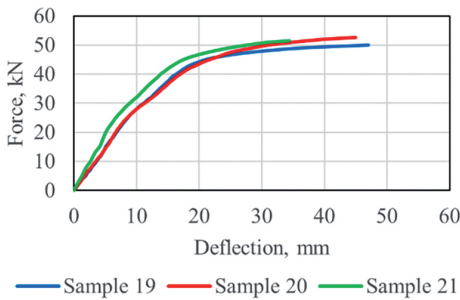
Fig. 15. Force – deflection curve for the type 3.1 joint. Bending about Y axis
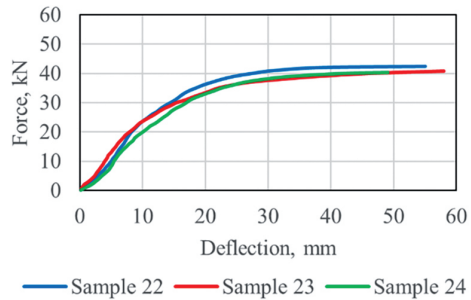
Fig. 16. Force – deflection curve for the type 3.1 joint. Bending about Z axis

In the case of the joint samples of type 3.1, the critical load point of the joints was recorded for the force value of 40 kN and 22 kN in the case of bending in the direction of higher and lower stiffness, respectively. Fig. 17 shows the samples of the type 3.1 joints after their failure.

The graphs of the dependence between the deflection of the samples of the 3.2 type joints and the force applied on them are presented in Fig. 18 and Fig. 19. The critical load

(a)

(b)

Fig. 17. Samples of the type 3.1 joint: (a) failure due to the plasticization of the material and the breaking of the most outer bolt, (b) the opening of the joint plates after failure
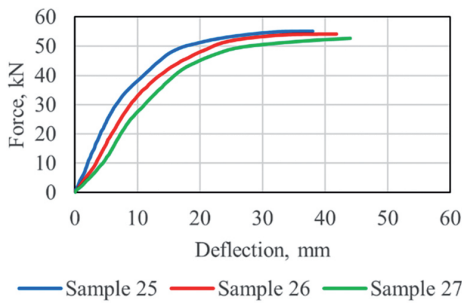
Fig. 18. Force – deflection curve for the type 3.2 joint. Bending in the about Y axis
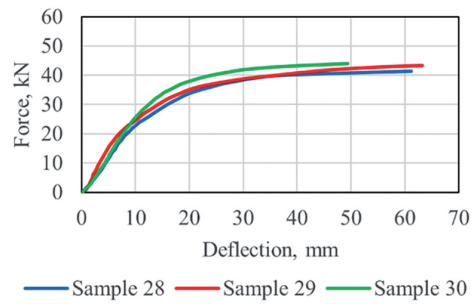
Fig. 19. Force – deflection curve for the type 3.2 joint. Bending about Z axis

point of the joint can be observed for the force value of 40 kN in the case of bending about Y axis, and for the force value of 23 kN while bending about Z axis.

Tested sample No. 28 was destroyed as a result of plasticization and the opening of the end-plates, followed by the breaking of the most outer bolt. In turn, the remaining samples were damaged due to the plasticization of the end-plates and the opening of the joint. Breaking of the bolts was not observed, but instead only their deformation.

Fig. 20 and Fig. 21 show the force-deflection relationships for the type 4.1 joint samples. The critical load point of the joint can be observed for the force value of about 30 kN in the case of bending about Y axis, and for the force value of 20 kN about Z axis.

The failure of the type 4.1 joint samples was due to the interaction of the plasticization of the joint plates, the opening of the joint, and the plasticization of the bolts' material (samples No. 31, 35, 36), or due to the breaking of the most outer bolt in the case of the remaining samples.

The results of the test of the type 4.2 joint samples are shown in Fig. 22 and Fig. 23.
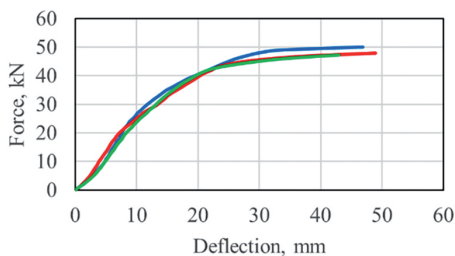
Fig. 20. Force – deflection curve for the type 4.1 joint. Bending about Y axis
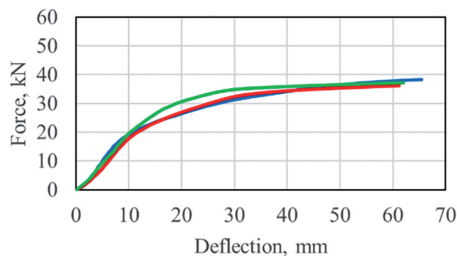
Fig. 21. Force – deflection curve for the type 4.1 joint. Bending about Z axis
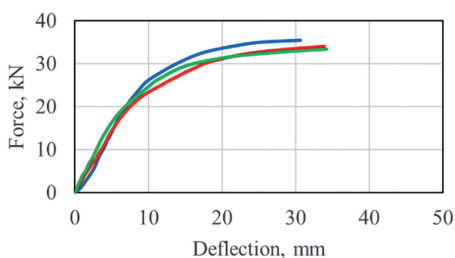
Fig. 22. Force – deflection curve for the type 4.2 joint. Bending about Y axis
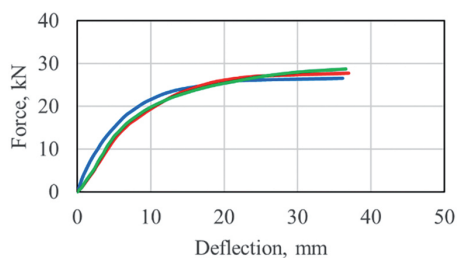
Fig. 23. Force – deflection curve for the type 4.2 joint. Bending about Z axis

The type 4.2 joint samples were damaged due to the opening of the joint between the end-plates, which was the result of the interaction of the plasticization of the joint plates and the most outer bolt. The critical load point of the joint was recorded for the force value of 21 kN and 15 kN in the case of bending in the direction of greater and lower stiffness, respectively.

Fig. 24 and Fig. 25 present a comparison of the averaged deflection values of the tested samples in relation to the force acting on them towards higher and lower stiffness, respectively.
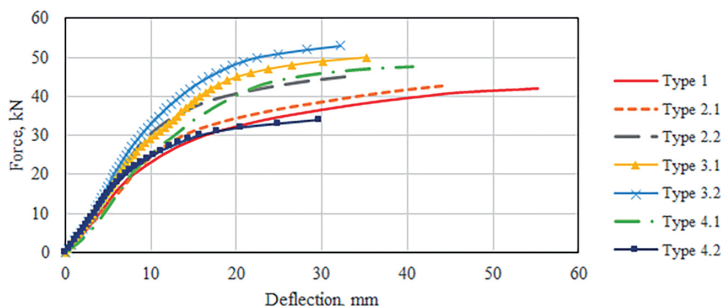
Fig. 24. Force – deflection curves for the tested joints – mean values. Bending in the Y direction
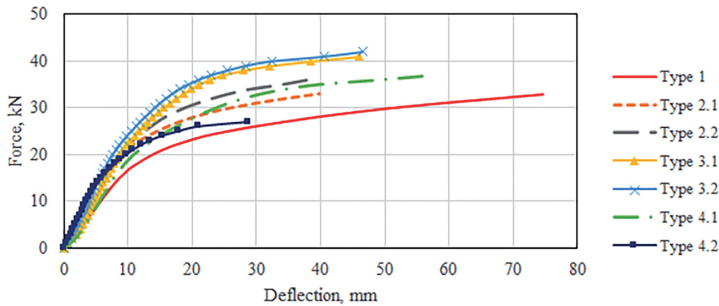
Fig. 25. Force – deflection curves for the tested joints – mean values. Bending in the Z direction

When analyzing the graphs in Fig. 24 and Fig. 25, it was noticed that:
– the samples of the profiles made of 4 mm metal sheet had a higher bearing resistance than the samples of the profiles made of 3 mm metal sheet,
– a higher bearing resistance was observed when using 5 bolts when compared to the use of 3 bolts,
– the use of class 10.9 bolts instead of the 8.8 class bolts allowed for the transferring of about a 4% greater bending moment.
– each of the tested joint samples of types 2.1 to 4.1 was characterized by a lower deflection when compared to the reference sample, while at the same time transmitting a greater bending moment. Only the type 4.2 samples had a reduced bearing resistance by about 20%, which was due to the use of the 3 mm thick metal sheet and 3 bolts.

4. Conclusions

As a result of the conducted tests, the influence of the variables (type of end-plates, number and class of bolts, thickness of the metal sheet of the joined profiles) on both the bending moment that the tested sample is able to transfer, and the accompanying deflection in the middle of the span of the prepared test beams, was determined.

When analyzing the test results (Table 2 and Table 3), it was observed that in the case of each of the tested samples (the joined profiles of which were made of 4 mm thick metal sheet), the bearing resistance of the joint was not less than the bearing resistance of the reference sample.

It was noticed that the percentage ratio of the bearing resistance of the tested type of joint in relation to the bearing resistance of the reference sample is similar in the case of carrying out tests in the directions of higher and lower profile stiffness.

It is important in the case of the performed tests to compare the bearing resistance of the modified samples with the bearing resistance of the reference sample. It was observed that the type 2.1 joint, made with the use of three M12 class 8.8 bolts, had a similar bearing resistance to that of the type 1 joint. It was equal to 10.7 kN·m in the direction of the greater

stiffness of the tested profile, and to 8.5 kN·m in the direction of its lower stiffness. Each of the subsequent tests was characterized by the transmission of a greater bending moment, with the greatest ability shown by the type 3.2 joint. The bearing resistance of this joint increased by about 26% in relation to the reference sample in both the tested directions.

Due to the much lower labor consumption and complexity of the 2.1–4.2 type joints (reference type of joint requires more material, more welding and is more complicated in prefabrication because end-plates need to be placed in a certain distance from the element edge before welding) and also a higher resistance, modified connections are recognized as suitable solution for use in modular structures.

Acknowledgements

References

[1] R.M. Lawson, R.G. Ogden, and R. Bergin, "Application of modular construction in high-rise buildings", *Journal of Architectural Engineering*, vol. 18, no. 2, pp. 148–154, 2012, doi: 10.1061/(ASCE)AE.1943-5568.0000057.

[2] H. T. Thai, T. Ngo, and B. Uy, "A review on modular construction for high-rise buildings", *Structures*, vol. 28, pp. 1265–1290, 2020, doi: 10.1016/j.istruc.2020.09.070.

[3] J. Olearczyk, M. Al-Hussein, and A. Bouferguene, "Evolution of the crane selection and on-site utilization process for modular construction multilifts", *Automation in Construction*, vol. 43, pp. 59–72, 2014, doi: 10.1016/j.autcon.2014.03.015.

[4] A. WA. Hammad, A. Akbarnezhad, P. Wu, X. Wang, and A. Haddad, "Building information modelling-based framework to contrast conventional and modular construction methods through selected sustainability factors", *Journal of Cleaner Production*, vol. 228, no. 10, pp. 1264–1281, 2019, doi: 10.1016/j.jclepro.2019.04.150.

[5] R. Alihodzic, V. Murgul, N. Vatin, E. Aronova, V. Nikolić, M. Tanić, and D. Stanković, "Renewable energy sources used to supply pre-school facilities with energy in different weather conditions", *Applied Mechanics and Materials*, vol. 624, pp. 604–612, 2014, doi: 10.4028/www.scientific.net/amm.624.604.

[6] J.Y.R. Liew, Y.S. Chua, and Z. Dai, "Steal concrete composite systems for modular construction of high-rise buildings", *Structures*, vol. 21, pp. 135–149, 2019, doi: 10.1016/j.istruc.2019.02.010.

[7] S. Mills, D. Grove, and M. Egan, "Breaking the pre-fabricated ceiling: Challenging the limits for modular high-rise", in *New York Conference Proceedings of CTBUH International Conference*. New York, USA: Council on Tall Buildings and Urban Habitat, 2015, pp. 416–425.

[8] W. Pan, Y. Yang, and L. Yang, "High-rise modular building: Ten-year journey and future development", in *Construction Research Congress*. New Orleans, Louisiana, USA: ASCE, 2018, pp. 523–532.

[9] N. Bertram, S. Fuchs, J. Mischke, R. Palter, G. Strube, and J. Woetzel, *Modular construction: From projects to products*. Warszawa: McKinsey & Company: Capital Projects & Infrastructure, 2019.

[10] A. Jellen, and A. Memari, "The state-of-the-art application of modular construction to multi-story residential building", in *Proceedings of the 1st Residential Building Design & Construction Conference*. Bethlehem, Palestine, 2013, pp. 284–293.

[11] A. W. Lacey, W. Chen, H. Hao, and K. Bi, "Structural response of modular buildings – An overview", *Journal of Building Engineering*, vol. 16, pp. 45–56, 2018, doi: 10.1016/j.jobe.2017.12.008.

[12] M. Lawson, R. Ogden, and C. Goodier, *Design in Modular Construction*. Boca Raton, USA: CRC Press, 2014.

[13] J. Peng, C. Hou, and L. Shen, "Numerical analysis of corner-supported composite modular buildings under wind actions", *Journal of Constructional Steel Research*, vol. 187, art. no. 106942, 2021, doi: 10.1016/j.jcsr.2021.106942.

[14] Y. Chen, C. Hou, and J. Peng, "Stability study on tenon-connected SHS and CFST columns in modular construction", *Steel and Composite Structures*, vol. 30, no. 2, pp. 185–199, 2019, doi: 10.12989/scs.2019.30.2.185.

[15] Z. Pisarek, "Obliczanie doczołowych połączeń śrubowych zginanych ukośnie", *Journal of Civil Engineering, Environment and Architecture*, vol. 60, no. 2, pp. 219–229, 2013, doi: 10.7862/rb.2013.27.

[16] H. Agerskov, "High-strength bolted connections subject to prying", *Journal of Structural Division*, vol. 102, no. 1, pp. 161–175, 1976, doi: 10.1061/JSDEAG.0004253.

[17] B. Kato and A. Mukai, "Bolted tension flanges joining square hollow section members", *Journal of Constructional Steel Research*, vol. 5, no. 3, pp. 163–177, 1985, doi: 10.1016/0143-974X(85)90001-X.

[18] A. Wheeler, M. Clarke, and G. J. Hancock, *Design model for bolted moment end-plate connections joining rectangular hollow sections using eight bolts. Research Report No R827*. Sydney, NSW, Australia: Department of Civil Engineering, The University of Sydney, 2003.

[19] M. Heinisuo, V. Laine, and E. Lehtimäki, "Enlargement of the component method into 3D", in *Nordic Steel Construction Conference, 2–4 September 2009, Malmö*, Sweden. 2009, pp. 430–437.

[20] N. Neumann and F. Nuhic, "Design of structural joints connecting H or I sections subjected to in-plane and out-of-plane bending", in *Proc. 6th European Conference on Steel and Composite Structures (Eurosteel 2011)*, vol. A. Budapest, 2011, pp. 303–308.

[21] N. Neumann, M. Buzaljkob, E. Thomassenc, and F. Nuhic, "Verification of design model for out-of-plane bending of steel joints connecting H or I sections", in *Proc. Nordic Steel Construction Conference (NSCC 2012)*. Oslo, 2012, pp. 683–692.

[22] PN-EN 1993-1-8 Eurokod 3: Projektowanie konstrukcji stalowych. Część 1–8: Projektowanie węzłów. PKN, 2005.

[23] W. Wuwer and R. Walentyński, "Analysis of a lap-joint in a thin walled structure under combined bending and shearing load", *Architecture Civil Engineering Environment*, vol. 3, no. 2, pp. 71–81, 2010.

[24] E. Bernatowska and L. Ślęczka, "Numerical study of block tearing failure in steel angles connected by one leg", *Archives of Civil Engineering*, vol. 67, no. 1, pp. 269–283, 2021, doi: 10.24425/ace.2021.136473.

[25] E. Bernatowska and L. Ślęczka, "Net section resistance of steel angles connected by one leg", *Archives of Civil Engineering*, vol. 68, no. 4, pp. 275–291, 2022, doi: 10.24425/ace.2022.143038.

Analiza nośności zmodyfikowanych śrubowych złączy doczołowych profili cienkościennych stosowanych w budownictwie modułowym

Słowa kluczowe: konstrukcja modułowa, nośność konstrukcji, profile cienkościenne, węzły konstrukcji modułowej

Streszczenie:

W pracy przedstawiono wyniki badań nośności połączeń, skręcanych profili cienkościennych wykorzystywanych w budownictwie modułowym. W badaniach wykorzystano dwa typy połączeń obecnie stosowanych w budownictwie, z których jedno posłużyło jako próba odniesienia, natomiast drugie jako próba badawcza mająca na celu znalezienie rozwiązania korzystniejszego pod względem złożoności procesu produkcyjnego oraz nośności połączenia. Oprócz zmodyfikowanego

kształtu blach czołowych, dokonano również analizy nośności połączenia w zależności od wykorzystanych różnych średnic śrub (stosowano śruby M12 oraz M16), jak również ich klasy (zbadano różnicę pomiędzy śrubami klasy 8.8 i 10.9) i ilości w połączeniu (3 lub 5 śrub). Ponadto w badaniach wykorzystano dwie grubości blach stalowych, z których wykonano łączone zimnogięte profile cienkościenne (3 mm i 4 mm). Próby nośności przeprowadzono z wykorzystaniem prasy wytrzymałościowej własnej konstrukcji. Na podstawie pomiarów sporządzono wykresy zależności ugięcia próbek od działającej w środku ich rozpiętości siły. Wykazano, że badane połączenie profili spowodowało wzrost ich nośności nawet o 26% w stosunku do próby odniesienia. Maksymalny niszczący moment zginający M wynosił 10,7 kN·m w przypadku próbki odniesienia oraz 13,5 kN·m w przypadku analizowanego rozwiązania konstrukcyjnego. Łącznie do testów wykonano 6 typów połączeń modyfikowanych, z czego 5 z nich wykazało nośność porównywalną, lub wyższą od próby odniesienia. Każdy z typów połączenia badano poprzez zginanie w dwóch kierunkach, względem osi centralnych przekroju.